High speed switching between arbitrary spatial light profiles

N. Radwell,* D. Brickus, T. W. Clark and S. Franke-Arnold

SUPA, School of Physics and Astronomy, University of Glasgow, Glasgow G12 8QQ, UK

**neal.radwell@glasgow.ac.uk*

Abstract: Complex images, inscribed into the spatial profile of a laser beam or even a single photon, offer a highly efficient method of data encoding. Here we present a prototype system which can quickly modulate between arbitrary images. We display an array of holograms, each defined by its phase and intensity profile, on a spatial light modulator. The input beam is then steered by an acousto-optic modulator to one of these holograms, where it is converted into the desired light mode. We demonstrate switching between characters within three separate alphabets at a switching rate of up to10 kHz. This rate is limited by our detection system, and we anticipate that the system is capable of far higher rates. Furthermore our system is not limited in efficiency by channel number, making it ideal for quantum communication applications.

OCIS codes: (230.1040) Acousto-optical devices; (270.5565) Quantum communications; (270.5585) Quantum information and processing.

References and links

1. C. Vitelli, N. Spagnolo, L. Aparo, F. Sciarrino, E. Santamato, and L. Marrucci, "Joining the quantum state of two photons into one," Nature Photonics **7**, 521–526 (2013).
2. M. I. Kolobov and C. Fabre, "Quantum limits on optical resolution," Phys. Rev. Lett. **85**, 3789 (2000).
3. G. Brida, M. Genovese, and I. R. Berchera, "Experimental realization of sub-shot-noise quantum imaging," Nature Photonics **4**, 227–230 (2010).
4. G. Molina-Terriza, J. P. Torres, and L. Torner, "Twisted photons," Nature Physics **3**, 305–310 (2007).
5. D. L. Andrews and e. Mohamed Babiker, *The Angular Momentum of Light* (Cambridge University Press, 2012).
6. A. Mair, A. Vaziri, G. Weihs, and A. Zeilinger, "Entanglement of the orbital angular momentum states of photons," Nature **412**, 313–316 (2001).
7. J. Leach, M. J. Padgett, S. M. Barnett, S. Franke-Arnold, and J. Courtial, "Measuring the orbital angular momentum of a single photon," Phys. Rev. Lett. **88**, 257901–257901 (2002).
8. R. W.Boyd, A. Jha, M. Malik, C. OSullivan, B. Rodenburg, and D. J.Gauthier, "Quantum key distribution in a high-dimensional state space: exploiting the transverse degree of freedom of the photon," Proceedings of the SPIE **7948**, 79480L (2011).
9. A. C. Dada, J. Leach, G. Buller, M. J. Padgett, and E. Andersson, "Experimental high-dimensional two-photon entanglement and violations of generalized bell inequalities," Nature Physics **7**, 677–680 (2011).
10. M. P. Lavery, D. J. Robertson, A. Sponselli, J. Courtial, N. K. Steinhoff, G. A. Tyler, A. E. Willner, and M. J. Padgett, "Efficient measurement of an optical orbital-angular-momentum spectrum comprising more than 50 states," New J. Phys. **15**, 013024 (2013).
11. J. Romero, D. Giovannini, S. Franke-Arnold, S. M. Barnett, and M. J. Padgett, "Increasing the dimension in high-dimensional two-photon orbital angular momentum entanglement," Phys. Rev. A **86**, 012334 (2012).
12. D. Giovannini, F. M. Miatto, J. Romero, S. M. Barnett, J. P. Woerdman, and M. J. Padgett, "Determining the dimensionality of bipartite orbital-angular-momentum entanglement using multi-sector phase masks," New J. Phys. **14**, 073046.
13. R. Fickler, R. Lapkiewicz, W. N. Plick, M. Krenn, C. Schaeff, S. Ramelow, and A. Zeilinger, "Quantum entanglement of high angular momenta," Sceince **338**, 640–643 (2012).

#207822 - $15.00 USD Received 11 Mar 2014; revised 2 May 2014; accepted 5 May 2014; published 20 May 2014

14. N. Bozinovic, Y. Yue, Y. Ren, M. Tur, P. Kristensen, H. Huang, A. E. Willner, , and S. Ramachandran, "Terabit-scale orbital angular momentum mode division multiplexing in fibers," Science **340**, 1545–1548 (2013).
15. J. Wang, J.-Y. Yang, I. M. Fazal, N. Ahmed, Y. Yan, H. Huang, Y. Ren, Y. Yue, S. Dolinar, M. Tur and A. E. Willner, "Terabit free-space data transmission employing orbital angular momentum multiplexing," Nature Photonics **6**, 488–496 (2012).
16. C. Polycarpou, K. N. Cassemiro, G. Venturi, A. Zavatta, and M. Bellini, "Adaptive detection of arbitrarily shaped ultrashort quantum light states," Phys. Rev. Lett. **109**, 053602 (2012).
17. D.J.Richardson, J.M.Fini, and L.E.Nelson, "Space-division multiplexing in optical fibres," Nature Photonics **7**, 354–362 (2013).
18. G. Thalhammer, R. W. Bowman, G. D. Love, M. J. Padgett, and M. Ritsch-Marte, "Speeding up liquid crystal slms using overdrive with phase change reduction," Optics express **21**, 1779–1797 (2013).
19. Y. Li, J. Kim, and M. J. Escuti, "Orbital angular momentum generation and mode transformation with high efficiency using forked polarization gratings," Applied optics **51**, 8236–8245 (2012).
20. M. Mirhosseini, O. S. Magana-Loaiza, C. Chen, B. Rodenburg, M. Malik, and R. W. Boyd, "Rapid generation of light beams carrying orbital angular momentum," Optics Express **21**, 30196–30203 (2013).
21. L. Marrucci, C. Manzo, and D. Papar, "Optical spin-to-orbital angular momentum conversion in inhomogeneous anisotropic media," Phys. Rev. Lett. **96**, 163905 (2006).
22. S. Slussarenko, E. Karim, B. Piccirillo, L. Marrucci, and E. Santamato, "Efficient generation and control of different-order orbital angular momentum states for communication links," JOSA A **28**, 61–65 (2011).
23. M. Mestre, B. V. de Lesegno, R. Farcy, L. Pruvost, J. Bourderionnet, A. Delboulbé, B. Loiseaux, and D. Dolfi, "Fast reconfigurable and transient-less holographic beam-shaping realized by a aom-slm device," Euro. Phys. J. Appl. Phys. **40**, 269 (2007).
24. G. C. G. Berkhout, M. P. J. Lavery, J. Courtial, M. W. Beijersbergen, and M. J. Padgett, "Efficient sorting of orbital angular momentum states of light," Phys. Rev. Lett. **105**, 153601 (2010).
25. N. J. Cerf, M. Bourennane, A. Karlsson, and N. Gisin, "Security of quantum key distribution using d-level systems," Phys. Rev. Lett. **88**, 127902 (2002).
26. S. Etcheverry, G. Cañas, E. S. Gómez, W. A. T. Nogueira, C. Saavedra, G. B. Xavier, and G. Lima, "Quantum key distribution session with 16-dimensional photonic states," Scientific Reports **3**, 2316 (2002).
27. B. P. Lanyon, M. Barbieri, M. P. Almeida, T. Jennewein, T. C. Ralph, K. J. Resch, G. J. Pryde, J. L. O'Brien, A. Gilchrist, and A. G. White, "Simplifying quantum logic using higher-dimensional hilbert spaces," Nature Physics **5**, 134–140 (2009).

1. Introduction

An increase in data capacity is one of the most pressing goals in both classical and quantum communication systems. For optical communication, this can be achieved either by increasing the number of transmitted photons, and/or by transmitting more than one bit (or qubit) per photon, i. e. encoding in an enlarged communication 'alphabet.' The latter corresponds to an increase in the number of orthogonal modes in which data is encoded [1]. Complex images can be used as one such set of orthogonal modes and have been shown to be highly efficient in storing data [2,3]. A particularly convenient subset of orthogonal light modes are those defined by their orbital angular momentum (OAM) [4–7], advocated in many recent fundamental and technological proposals on high dimensional light processing [8–10]. OAM modes are characterised by their azimuthally varying phase around a central vortex line. They offer a theoretically infinite dimensional state space, and the generation of large OAM values up to several hundred has been demonstrated [11–13].

In order to fully access the benefit of such multimode communication for commercially viable systems, one would require elements that can rapidly encode and decode light in modes with different spatial profiles.

For classical communication systems, multiplexing of OAM modes has recently led to record-breaking data communication rates in the terabit regime [14,15], and fast space-division multiplexing was achieved in fibre based applications [16,17]. These systems, however, rely on distinct communication channels for each spatial light mode, with an associated laser and detection system, thereby operating at an efficiency that scales inversely with the number of OAM channels. Multiplexing along N channels thus results in a signal strength of $1/N$, prohibiting efficient operation in the quantum regime.

#207822 - $15.00 USD Received 11 Mar 2014; revised 2 May 2014; accepted 5 May 2014; published 20 May 2014

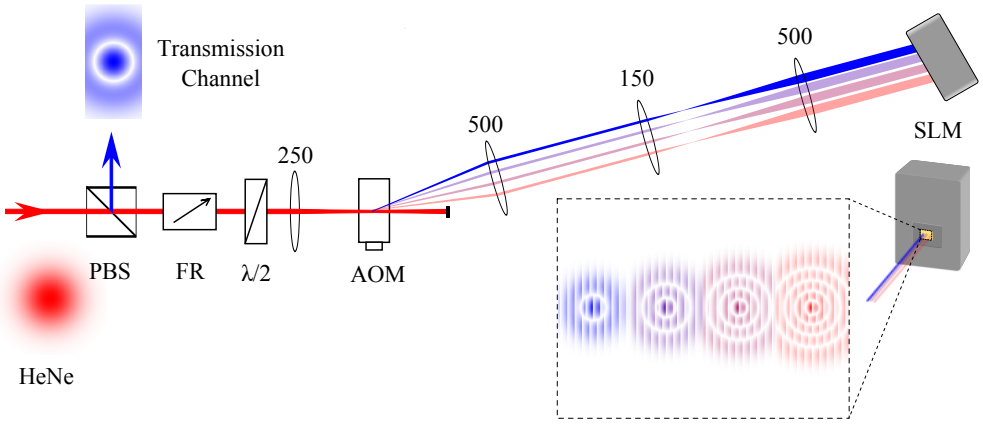

Fig. 1. Experimental setup. HeNe: helium neon laser, PBS: polarising beam splitter, FR: Faraday rotator, $\lambda/2$: half-wave plate, AOM: acousto optic modulator, SLM: spatial light modulator. The focal lengths of the lenses are given in millimetres. The four beams exiting the AOM indicate the effect of changing the drive frequency of the AOM. The inset picture shows a false colour image of a sample hologram array displayed on the SLM. Steering along the blue path to the left-most hologram produces the shown output mode in the transmission channel.

Conventional OAM generating systems, including spatial light modulators (SLMs) [18] and polarisation based liquid crystal devices [19] are limited to switching rates of at best 1 kHz. Faster rates have been obtained by using digital micromirror devices (DMD) [20] or by combining q-plates [21] with electro-optical modulators, but the generalisation to higher dimensions requires a multistage setup which places limits on scalability [22].

Here we present a prototype system capable of fast and efficient switching between arbitrary complex light profiles, transmitted along a single channel. In particular, our system does not suffer from the typical $1/N$ scaling, making it suitable for the encryption of individual photons for quantum communication applications.

2. Experimental details

Our system contains a fixed component, defining the communication alphabet, and a fast component, addressing the individual letters. The alphabet is defined by an array of holograms, with each individual hologram encoding one of the letters. For convenience, we display the hologram array on an SLM (Hamamatsu LCOS), acting as a programmable diffraction grating, however this could instead be replaced by a custom designed fixed hologram. Fast switching between the different letters is achieved with an Acousto-Optic Modulator (AOM, Crystal Technology 3080-122, central modulation frequency 80 MHz) which deflects the input beam towards one of the holograms and, crucially, switches between them at a rate determined by the AOM rise time and driving electronics. We note that a similar system was employed by Mestre et. al. [23] in the context of trap shaping for use in optical tweezers and atom traps.

Our experimental setup, shown in Fig. 1, is based on an extended double-pass AOM configuration. This configuration provides a fixed communication channel by keeping the angle and position of the output beam constant for all encoded letters. The hologram array offers flexibility in defining alphabets generated from any arbitrary intensity and phase profiles.

At the input of the system, a linearly polarised helium neon laser enters through a polarising

#207822 - $15.00 USD Received 11 Mar 2014; revised 2 May 2014; accepted 5 May 2014; published 20 May 2014

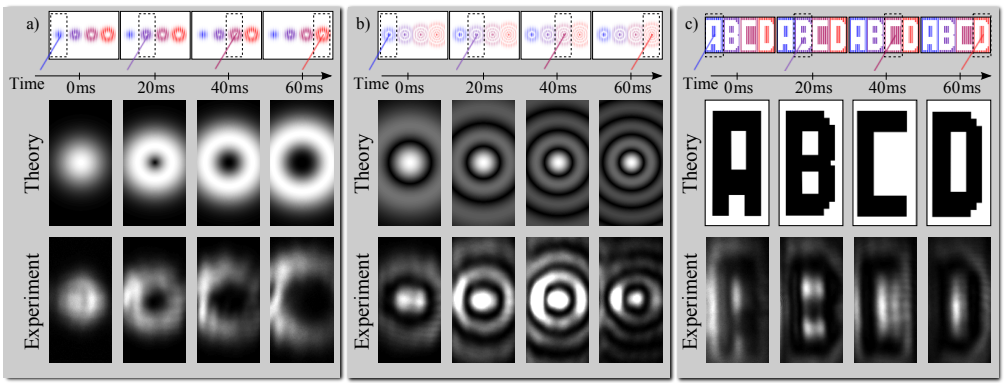

Fig. 2. Hologram arrays, theoretical predictions and beam profiles for three different communication alphabets. The alphabet in a) has an azimuthal number l, varying from 0 to 3 and b) has a radial number p varying from 1 to 4. The alphabet in c) consists of the Latin characters 'A' to 'D.' The top row shows the (false colour) holograms for each alphabet and the time at which the beam is switched to that hologram. The middle row shows the expected intensity in the output channel when the beam is shone on the portion of the hologram shown above. The bottom row shows the corresponding experimental data. The data in the bottom row of a) and c) has been intensity scaled such that the maximum intensity is white. The data in the bottom row of b) for the p=2, 3 and 4 modes has been enhanced by a factor 2, 3 and 4 respectively to emphasise the low intensity features.

beamsplitter, and after passing through a sequence of polarisation optics, is focused into the AOM (waist size 150 μm). There the beam is deflected by an angle which is controlled by the AOM drive frequency. The beam is then collimated and magnified such that it slightly overfills one individual hologram and can be deflected to sample the whole alphabet displayed on the SLM. The first order diffracted beam is encoded with the complex spatial profile defined by the hologram of the particular sampled letter. The SLM is aligned so that the deflected beam retraces its path through the system and upon returning to the AOM the beam acquires a second, reverse angle shift such that it further retraces its path, regardless of the steering imposed by the AOM. A Faraday rotator ensures that the beam leaves the system via the output port of the polarising beamsplitter. Light in this transmission channel can therefore be modulated in its complex profile by changing the AOM drive frequency.

The hologram array is displayed on an SLM with a resolution of 800 x 600 pixels and 20 μm pixel size. The hologram for each letter is generated by the combination of three patterns. The first is a linear phase ramp which creates a grating. This is then added to the phase profile of the desired letter, generating the required phase in the first order of the linear diffraction grating. The modulation depth of the grating can further be modified to tune the intensity of the light in this first order, allowing full control over phase and intensity. The SLM is then positioned at an angle such that the first diffracted order is exactly counterpropagating with respect to the input beam (Littrow configuration).

The AOM deflection angle varies with input drive frequency at 0.19 mrad/MHz, with a usable bandwidth of 40MHz (60 MHz - 100 MHz modulation frequency), and therefore a total deflection range of 7.9 mrad. We note that in our current system different letters are associated with a different frequency sideband of the incoming light, with the frequency of the output beam shifted by twice the drive frequency of the AOM.

In order to separate the incoming beam from the output beam, we use a series of polarisation optics. The beam enters via a polarising beam splitter and is then rotated in its polarisation by

#207822 - $15.00 USD Received 11 Mar 2014; revised 2 May 2014; accepted 5 May 2014; published 20 May 2014

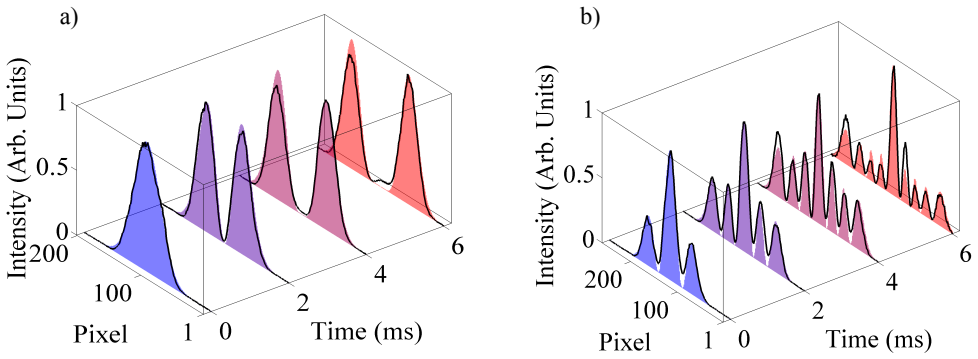

Fig. 3. CCD line profiles of the output beam as the AOM directs the beam to 4 different holograms. The data is displayed as solid lines, and the coloured fill shows an ideal LG mode, corrected for the Gaussian profile of the beam incident on the SLM; a) LG modes with $l = 0$, 1, 2 and 3 units of orbital angular momentum (left to right), all with $p = 0$. b) LG modes defined by their radial quantum number $p = 1$, 2, 3 and 4 (left to right), all with $l = 0$.

45° with a Faraday rotator. A subsequent half wave plate ensures that the beam is horizontally polarised, which is required for optimal operation of the SLM. After reflection from the SLM, the beam returns to the Faraday rotator and experiences a second rotation of 45°, thereby forcing the beam to exit through the other polarising beam splitter port into the transmission channel.

3. Results

We illustrate the ability of the system to switch between spatially encoded states using three different communication alphabets, each consisting of four letters. The first two are subsets of the complex profiles of Laguerre-Gaussian (LG) modes, while the third communication alphabet contains the first four characters of the Latin alphabet, 'A' to 'D,' shown in Fig. 2(a), 2(b) and 2(c) respectively. LG modes are parameterised by their winding number l, specifying their OAM content, and their radial mode number p. As all LG modes are orthogonal, any subset presents a possible alphabet. Here we use subsets specified only by l, and p respectively.

We set the SLM to display one of the hologram arrays in the top row of Fig. 2 and monitor the output in the communication channel on a standard CCD camera. The predicted intensity profiles (middle row) and the measured profiles (bottom row) show good qualitative agreement, in particular of the defining modal lines. The imperfections are believed to be due to astigmatism associated with passing through the AOM crystal and minor system misalignment. We note that LG modes are highly sensitive to aperturing, e. g. through the limited size of the AOM crystal. With this in mind the alignment and focusing parameters were adjusted very carefully to minimise such effects.

As previously stated, one of the advantages of our system is the capability to produce arbitrary phase and intensity profiles, and not only eigenmodes of propagation such as the LG modes. Here we concentrate on an intensity modulation. In our experiment, the SLM plane is imaged onto the output plane. This allows us to write arbitrary dark shapes within the beam profile by dimming the local contrast of the diffraction grating, or simply by removing individual pixels from the displayed hologram pattern. We demonstrate this by generating the letters A, B, C and D, with results shown at the bottom of Fig. 2(c).

The time resolution at which we can demonstrate switching between different light profiles

#207822 - $15.00 USD Received 11 Mar 2014; revised 2 May 2014; accepted 5 May 2014; published 20 May 2014

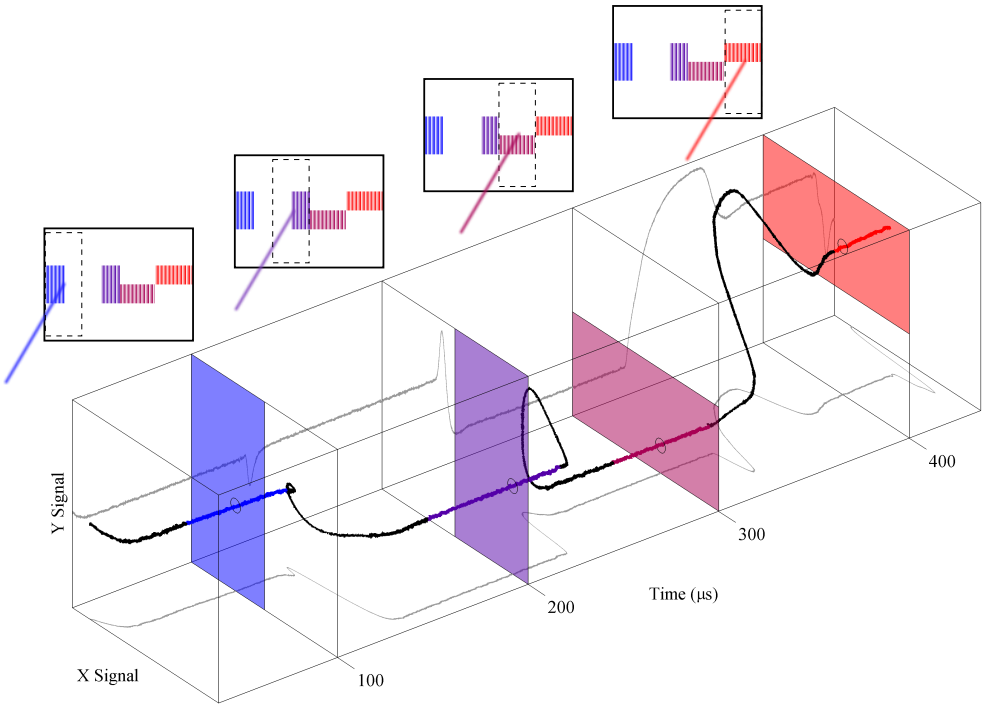

Fig. 4. Trajectory of the QPD signal in time. The x and y signals are taken directly from the QPD and plotted vs. time. The semi-transparent planes indicate the pattern in which the beam is shaped at a particular time. The colored parts of the trajectory indicate the regions in which the output is stable at the desired location. The grey projected lines are the projection of the trajectory onto the axes. The hologram arrays shown above correspond to the patterns displayed on the SLM as the 'simplified alphabet.'

is limited by the detection rate of the CCD camera rather than the generation rate. To test the system at higher speeds and to obtain more quantitative results we restrict the CCD image to a single line of pixels. These 1D-profiles of the LG-based alphabets, taken at 500 Hz, are shown in Fig. 3(a) and 3(b) together with a theoretical prediction of the beam shapes. In particular the positions of the modal lines are highly accurate, resulting in a very clear distinction between the different p and l modes.

In order to increase the detection speed beyond that allowed by standard CCD cameras, we replaced the camera with a quadrant photodiode (QPD, New Focus 2901). The device outputs directly an x (y) signal, which internally is the difference between both left (upper) and both right (lower) quadrants. These x and y coordinates give the centre of mass of an incident beam and can be read at up to 100 kHz, however the signal quality is already significantly diminished at this rate. We have devised a different communication alphabet, suitable for detection with the QPD, consisting of very simple 'letters.' These letters are the left, right, lower and upper half of the input beam respectively and they can be generated by deflecting only the corresponding halves of the beam using the holograms shown in the insets of Fig. 4. Each letter is designed to fill two quadrants of the QPD, as this results in a higher signal to noise ratio compared to the illumination of a single quadrant.

We switch between these simplified letters at 10 kHz by steering the input beam via the AOM to the corresponding holograms as before. We record the signal position in x and y as a function

#207822 - $15.00 USD Received 11 Mar 2014; revised 2 May 2014; accepted 5 May 2014; published 20 May 2014

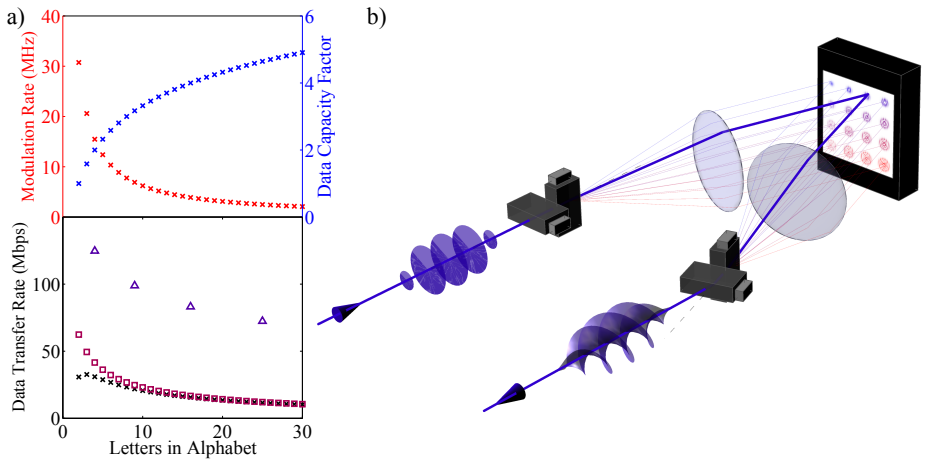

Fig. 5. a) Predicted system performance as a function of the alphabet size. Top: Estimated modulation rate (red curve) and data capacity (blue) for the used system in Fig. 1. Bottom: Resulting data transfer rate considering delay due to AOM switching and propagation (crosses), and for a system without propagation delay for a 1D (squares) and 2D (triangles) hologram array. b) Schematic diagram of a proposed experimental setup for larger alphabets which avoids propagation delay. The encoded beam is shown for $l = 3$ and $p = 0$.

of time, displayed as a 3D trajectory in Fig. 4. The QPD signal alternates between transient switching phases and phases of stable beam position, each lasting $\sim 100\mu$s. This confirms that our system operates successfully near the maximum QPD detection bandwidth, which, we note, is still orders of magnitude below the expected generation limit. Faster measurements are beyond our current experimental scope but could involve the use of ultrafast cameras, an LG modesorter [24], SLMs linked to avalanche photodiodes, or even the encoder introduced here, run in reverse as a decoder.

4. Discussion of system performance

The efficiency of the system is limited by the diffractive elements, with $\sim 85\%$ per diffraction for both the SLM and the AOM. Double passing the AOM and a single diffraction from the SLM results in $\sim 61\%$ efficiency for the entire system. We note that our system avoids the typical $1/N$ intensity scaling for N modes in conventional multiplexing. This results in scalability to large alphabets with no loss of efficiency, making the system particularly attractive for single photon communication applications.

In the following we discuss the potential data transfer rate that can be achieved with the system considered here and suggest ways to avoid the identified design limitations. The data transfer rate of the system is reliant primarily on two factors; the modulation rate of the signal and the data capacity of each signal. The modulation rate depends on the rise time of the AOM and the photon transit time from the AOM to the SLM and back. The rise time varies with the beam size in the AOM and the transit time with the length of the optical system, which are both dictated by the constituent lenses. The data capacity can be increased by increasing the number of letters in the alphabet. This is quantified by a 'data capacity factor' of $\log_2(A_s)$ where A_s is the number of letters in the alphabet, such that the data capacity factor represents the number of bits required to contain the same amount of data. Larger alphabets require a smaller beam size at the SLM and because the SLM and AOM are in conjugate Fourier planes this leads to larger beam waists in the AOM and therefore slower modulation rates, so that an increase in

#207822 - $15.00 USD Received 11 Mar 2014; revised 2 May 2014; accepted 5 May 2014; published 20 May 2014

data capacity is associated with a decrease in modulation rate as shown in the top of Fig. 5(a).

The total data transfer rate is then the product of these two factors, shown in the lower part of Fig. 5(a). The rate achievable in our current system (crosses) peaks for 3 and 4 letters in the alphabet. This rate can be increased in two ways: by removing the photon transit time and by defining the alphabet as a 2D array of holograms rather than a linear array. A setup which can achieve this is proposed in Fig. 5(b). Transmission through two perpendicular AOMs allows steering in two dimensions. Rather than backtracing the encoded beam through the system it could be steered toward the output channel by a further two AOMs driven at the same frequency as those in the input, with an appropriate delay. Potential data transfer rates are shown in the lower part of Fig. 5(a) for a 1D (squares) and a 2D (triangles) hologram array.

The previous anlysis holds for the case in which the highest possible efficiencies are desired however there is flexibility to increase the data rate at the cost of efficiency. The modulation rate is highest when the beam is largest at the SLM and thus if one may tolerate the overlapping of the input beam onto several hologram sections then higher data rates may be achieved. The output must then be spatially filtered, reducing the efficiency of the system leading to the well-known $1/N$ type efficiency found in other multiplexing systems.With this approach, expanding the beam to fill the SLM and using a 4×4 hologram array would lead to data rates of close to 1 Gbps.

Following these considerations it is then possible to design an optical system which is either optimised for high efficiency, ideal for single photon experiments, or optimised for high speed operation at the expense of efficiency, more suited for classical communication.

5. Conclusion

In conclusion we have developed a prototype encoder which is capable of rapidly switching between the letters of an arbitrary communication alphabet. We have demonstrated switching between alphabets based on a different phase and intensity profiles, including OAM based alphabets. The modulation rate in our prototype system has been verified up to 10 kHz, limited by our detection bandwidth. With more advanced detection systems and optimisation of the driving electronics we predict high speed encoding at rates that exceed 20 MHz. We anticipate applications in communication protocols involving complex images, and in particular in high-dimensional quantum communication [8, 25–27].

Acknowledgments

This work was supported by the Engineering and Physical Sciences Research Council [grant number EP/I012451/1] and we acknowledge financial support by the European Commission via the FET Open grant agreement Phorbitech FP7-ICT-255914.

#207822 - $15.00 USD Received 11 Mar 2014; revised 2 May 2014; accepted 5 May 2014; published 20 May 2014